Experimental Neurology 317 (2019) 1–9

Contents lists available at ScienceDirect

Experimental Neurology

journal homepage: www.elsevier.com/locate/yexnr

Research Paper

Mitoquinone attenuates blood-brain barrier disruption through Nrf2/PHB2/OPA1 pathway after subarachnoid hemorrhage in rats

Tongyu Zhang[a,b,1], Shancai Xu[a,1], Pei Wu[a,b], Keren Zhou[b], Lingyun Wu[b], Zhiyi Xie[b], Weilin Xu[b], Xu Luo[b], Peng Li[b], Umut Ocak[b], Pinar Eser Ocak[b], Zachary D. Travis[c], Jiping Tang[b], Huaizhang Shi[a,*], John H. Zhang[b,*]

[a] Department of Neurosurgery, The First Affiliated Hospital of Harbin Medical University, Harbin, Heilongjiang, China
[b] Department of Physiology and Pharmacology, Loma Linda University, 11041 Campus St, Risley Hall, Room 219, Loma Linda, CA 92354, USA
[c] Department of Earth and Biological Sciences, Loma Linda University, Loma Linda, CA, USA

ARTICLE INFO

Keywords:
Mitoquinone
NF-E2-related factor 2
Prohibitin 2
Optic atrophy 1
Blood-brain barrier disruption
Subarachnoid hemorrhage

ABSTRACT

Background and purpose: Mitochondrial dysfunction is involved in the mechanism of early brain injury (EBI) following subarachnoid hemorrhage (SAH). Blood-brain barrier disruption is a devastating outcome in the early stage of SAH. In this study, we aimed to investigate the role of a mitochondria-related drug Mitoquinone (MitoQ) in blood-brain barrier disruption after SAH in rats.

Methods: A total of 181 male Sprague–Dawley SAH rats with the endovascular perforation model were utilized. Intraperitoneal MitoQ was given 1 h (h) post-SAH. Cerebroventricular ML385, an inhibitor of NF-E2-related factor 2 (Nrf2) and Small interfering ribonucleic acid (siRNA) for Prohibitin 2 (PHB2) were injected respectively 24 h and 48 h before SAH. Neurological function evaluation was performed before sacrifice. SAH grade was measured during the sacrifice of each animal. Brain water content was performed at 24 h. Co-immunoprecipitation was used to demonstrate the relationship of proteins Nrf2 and PHB2. Mitochondrial and cytoplasmic fractions were gathered using mitochondria isolation kits. Pathway related proteins were investigated with Western blot and immunofluorescence staining. Transmission electron microscopy was performed for mitochondrial morphology.

Results: Expression of Nrf2 levels peaked at the 3 h time point following SAH and then decreased to normal levels at 24 h, while PHB2 and Optic Atrophy 1 (OPA1) decreased at 24 h and 72 h after SAH compared with the Sham group. MitoQ treatment attenuated neurological deficits and brain edema, thereby resulting in a decreased expression of Albumin, while an increase of Nrf2, PHB2, OPA1 and Claudin-5 proteins compared with SAH + vehicle group. With co-immunoprecipitation, Nrf2 and PHB2 were further demonstrated to show their interaction. And MitoQ administration lead to more binding of the two proteins. ML385 abolished the effects of MitoQ on neurobehavior and protein levels post-SAH. Similarly, PHB2 siRNA reversed the neuroprotection of MitoQ administration with the decreased expression of PHB2 and OPA1 after SAH. Further, MitoQ treatment improved mitochondrial morphology after SAH with an increase of PHB2 and OPA1 in mitochondrial extraction.

Conclusions: MitoQ attenuates blood-brain barrier disruption via Nrf2/PHB2/OPA1 pathway after SAH in rats. MitoQ may serve as a potential therapeutic strategy for SAH patients.

1. Introduction

Subarachnoid hemorrhage (SAH) is a severe cerebrovascular disease with high rates of morbidity and mortality (Fujii et al., 2013). Blood brain barrier (BBB) disruption in the early stage of SAH is one of the most crucial mechanisms resulting in poor outcomes of SAH patients (Chen et al., 2014; Claassen et al., 2002). Recent studies reported that mitochondrial dysfunction is an underlying cause of BBB disruption in early brain injury (EBI) (Fan et al., 2017). Thus, an effective treatment for attenuation of mitochondrial injury would play an important role in therapeutic strategy for patients with SAH. Furthermore, mitochondrial dynamic improvement was reported to safeguard against neurological deficits after SAH (Wu et al., 2017; Zhang et al., 2018). However, the role of mitochondrial dynamics especially mitochondrial fusion in BBB

* Corresponding authors.
E-mail addresses: huaizhangshi@126.com (H. Shi), jhzhang@llu.edu (J.H. Zhang).
[1] Tongyu Zhang and Shancai Xu contributed equally to this work.

https://doi.org/10.1016/j.expneurol.2019.02.009
Received 13 December 2018; Received in revised form 11 February 2019; Accepted 15 February 2019
Available online 16 February 2019
0014-4886/

disruption after SAH is still unclear and needs to be further investigated.

Mitoquinone (MitoQ) is a mitochondrial-targeting drug, which contains several hundred-fold properties of aids in the prevention of mitochondrial dysfunction when compared with untargeted antioxidants (McManus et al., 2011). However, mechanisms of MitoQ treatment have never been investigated in the context of SAH. Furthermore, NF-E2-related factor 2 (Nrf2) has been identified to be a primary target of BBB disruption in various diseases, as well as in the SAH model (Gu et al., 2017; Yu et al., 2018). Although MitoQ has been reported to activate Nrf2 for autophagy in kidney injury (Xiao et al., 2017), it still needs to be investigated after induction of SAH. We postulate that the Nrf2 participates in the protective effect of MitoQ against BBB damage after induction of SAH.

Prohibitin 2 (PHB2), is a receptor located in the inner membrane of the mitochondria and is related to mitochondrial dynamics (Osman et al., 2009; Wei et al., 2017). PHB2's downstream protein Optic Atrophy 1 (OPA1) may improve the process of mitochondrial fusion in central nervous system (CNS) which cause neuroprotection in neurodegeneration (Korwitz et al., 2016). Our recent study further proved that enhance the expression of OPA1 may cause neuroprotection after SAH (Zhang et al., 2018). Recent study in ischemic stroke has proved that the association of Nrf2 to brain mitochondria was involved in astrocytes (Narayanan et al., 2018). Moreover, a recent study of hepatocarcinogenesis reported that the genes of Nrf2 and PHB2 are binding together for expression (Kakehashi et al., 2011). Thus, PHB2 may play a mediator role in the mechanism of BBB protection induced by MitoQ, which would be a worthwhile and a novel target to pursue for SAH.

Thus, we hypothesize that MitoQ will protect BBB via the Nrf2/PHB2/OPA1 pathway in EBI after SAH in rats (Supplemental Fig. I).

2. Material and methods

2.1. Animal and SAH model

Adult male Sprague–Dawley rats (n = 181, weight 280–320 g) were housed in a controlled humidity and room temperature with a 12 h light and dark cycle and were raised with free access to water and food. All experiments were approved by the Institutional Animal Care and Use Committee (IACUC) of Loma Linda University. During the entirety of the experiments, rats were cared for in accordance with the NIH Guide for the Care and Use of Laboratory Animals.

The SAH model was performed by the endovascular perforation as previously reported (Sugawara et al., 2008). Briefly, the rats were anesthetized with 3% isoflurane in 65/35% medical air/oxygen through tracheal intubation by a rodent ventilator (Harvard Apparatus, Holliston, MA, USA). Then A sharpened 4–0 monofilament nylon suture was inserted into the left internal carotid artery from the cut of external carotid artery stump until resistance was felt. The suture was advanced further to perforate the bifurcation of the left anterior and middle cerebral artery followed by immediate withdrawal. In sham-operated animals, the same procedures were performed except perforation with suture.

2.2. Drug administration

MitoQ was purchased from MedKoo Biosciences (pre-dissolved in a 1:1 ratio of an ethanol-water mixture, yielding a concentration of 200 mg/mL, Morrisville, NC) and it was dissolved in 1 mL 0.9% sterile NaCl and administered intraperitoneally (i.p.) 1 h after SAH. ML385 (50 pmol/5 μL; AOBIOUS, MA, USA) was diluted in DMSO before intracerebroventricular (i.c.v.) injection and administered 24 h before SAH. SAH + vehicle group and SAH + DMSO group received an equal volume of solvents respectively with SAH + MitoQ group and SAH + ML385 + MitoQ group. Three different formats of Prohibitin2 small interfering ribonucleic acid (PHB2 siRNA, 500 pmol/5 μL RNase-free water, OriGene Technologies, Rockville, MD, USA), scramble siRNA (Scr siRNA, 500 pmol/5 μL, OriGene Technologies, Rockville, MD, USA) was injected i.c.v. at 48 h pre-surgery. To enhance the gene silence efficiency, 3 different PHB2 siRNA were mixed, listed as follows: (1) 5'GAGCAAGAAUCCUGGCUAUAUCAAG3'; (2) 5'AUCAUGUGAUGGAUUCUUCUGUATC3'; (3) 5'AGCAUCAUGUGAUGGAUUCUUCUGT3'.

2.3. Intracerebroventricular administration

Intracerebroventricular drug administration was performed as previously described (Yan et al., 2011). Briefly, post-anesthetized rats were placed in a stereotaxic apparatus under 2% isoflurane anesthesia during the entirety of the surgery. A 10-μL Hamilton syringe (Microliter 701; Hamilton Company, Reno, NV) was delivered into the left ventricle through a burr hole at the following coordinates relative to bregma: 1.5 mm posterior, 1.0 mm lateral, and 3.2 mm below the dural surface. The drugs were injected at a rate of 0.5 μL/min. The needle was kept in place for 5 min after infusion and then slowly removed.

2.4. Experimental design (Supplemental Fig. II)

Experiment 1–36 rats were divided randomly into six groups (n = 6/group): Sham, SAH (3, 6, 12, 24, 72 h) groups. In addition, 3 Sham and 3 SAH (24 h) rats were used for immunofluorescence staining. The temporal expression of Nrf2, PHB2, and OPA1 was detected by Western blot. Immunofluorescence staining was performed to test the localization of Nrf2, PHB2, and OPA1 in the astrocytes and endothelial cells post-SAH.

Experiment 2–30 rats were divided randomly into five groups (n = 6/group): Sham, SAH + vehicle, SAH + MitoQ (1 mg/kg), SAH + MitoQ (3 mg/kg), and SAH + MitoQ (9 mg/kg). Based on neurological and brain water content tests, 3 mg/kg of the MitoQ-treated group of SAH was chosen for experiments 3 and 4.

Experiment 3–51 rats were divided randomly into seven groups: Sham, SAH + vehicle, SAH + MitoQ groups with n = 9 (including 3 rats for Co-immunoprecipitation, 6 rats for neurological tests and Western blot), SAH + ML385 + MitoQ, SAH + DMSO + MitoQ, SAH + PHB2 siRNA + MitoQ and SAH + Scr RNA + MitoQ groups with n = 6 (the relevance factors were utilized for neurological tests and Western blot).

Experiment 4–18 rats were randomly divided into three groups (n = 9/per group, including 3 rats for Transmission Electron Microscopy and 6 rats for mitochondrial extraction): Sham, SAH + vehicle, SAH + MitoQ groups. The mitochondrial components were gathered to test expressions of mitochondrial-related proteins with Western blot.

2.5. Severity of SAH

The severity of SAH was blindly measured using the SAH grading scale after euthanasia as previously described (Sugawara et al., 2008). Briefly, the ventral side of rat brains were photographed immediately after euthanasia and evaluated by an independent observer. The sum of six sub-scores based on six corresponding predetermined areas was calculated as the total score (maximum 18). Rats with SAH grading scores of ≤7 at 24 h were excluded from this study.

2.6. Assessment of neurobehavioral outcomes and brain water content

An 18-point scoring system with a modified Garcia scale and another 4- point scoring system with beam balance test were utilized to blindly evaluate as previous described (Pang et al., 2018). Briefly, the modified Garcia test sore (maximum 18) is composed of six subtests, including spontaneous activity, spontaneous movement of forelimbs, forelimbs outstretching, vibrissa touch, body proprioception, and climbing capacity. The beam balance score was evaluated from 0 to 4

according to the ability of animals walking on a narrow wooden beam in 1 min. The mean of three consecutive trials was calculated as the final score.

The brains in each group were harvested without clotted blood and perfusion, then weighed for brain water content as previously described (Sugawara et al., 2008). Each sample was weighed and recorded as wet weight (WW). Dry weight (DW) was obtained using a drying oven at 105 °C. The percentage of brain water content was calculated as [(WW − DW)/WW] × 100%.

2.7. Western blot

Left hemispheres of brain samples were collected 24 h after SAH. Western blot was performed as previously described (Chen et al., 2017). Briefly, equal amounts of protein samples with loading buffer were loaded into each lane of the SDS-PAGE gel. After electrophoresis, the protein samples were transferred onto a nitrocellulose membrane. Then the membrane was blocked with a blocking solution for 2 h. Next, the membrane was incubated overnight with primary antibody at 4 °C. The primary antibodies with dilution were listed as follows: anti-Nrf2 (1:1000, ab89443), anti-PHB2 (1:1000, ab15019), anti-OPA1 (1:5000, BD-612607), anti-Albumin (1:1000, ab106582), anti-Claudin 5 (1:1000, ab131259), anti-β-actin (1:5000, sc-517,582, used as loading control for total and cytoplasmic proteins). Appropriate secondary antibodies were all purchased from Santa Cruz Biotechnology (Dallas, TX) with a dilution of 1:5000. After incubation with selected secondary antibody for 2 h in room temperature, the membrane was colored with an ECL reagent (Amersham Biosciences UK Ltd., PA, USA). Detected blot bands were quantified by densitometry using Image J software (National Institutes of Health, Bethesda, MD).

2.8. Histomorphology measurement

Double immunofluorescence, A series of 8 μm slices were prepared in Sham and SAH + vehicle groups. Double immunofluorescence staining was performed as previously described (Chen et al., 2017). The region of interest was the left basal cortex-facing blood clots. Briefly, during euthanasia, rats were intracardially perfused with 60 mL ice-cold phosphate buffer (PBS) and 60 mL of 10% paraformaldehyde through the upper part of the body. The whole brain was then gathered and fixed in 10% paraformaldehyde for 24 h followed by 30% sucrose for three days. After freezing in −80 °C for 1 h, a series of 8 μm thick brain slices were cut on a cryostat (LM3050S; Leica Microsystems, Bannockburn, III, Germany). Double fluorescence labeling was processed with 0.3% Triton punching for 10 min, 5% donkey serum blocking for 1 h and the following primary antibody incubating overnight at 4 °C. primary antibodies: anti-Nrf2 (1:100; ab89443), anti-PHB2 (1: 200; ab15019), anti-OPA1 (1:200, BD-612607), anti-GFAP (1:200, ab53554) and anti-lectin (1:400, DL-1177) were used as primary antibodies. Appropriate fluorescence dye-conjugated secondary antibodies (1:500, Jackson Immunoresearch, West Grove, PA) were incubated for 2 h in room temperature before DAPI (Vector Laboratories, Inc., Burlingame, CA) staining and microscope observation (Leica Microsystems, Germany).

2.9. Co-immunoprecipitation

Pierce™ Co-Immunoprecipitation Kit from Thermo Fisher Scientific (Grand Island, NY, USA) was used for protein interactions as previously described (Yu et al., 2018). Briefly, precipitates were extracted from rat brains in Sham, SAH + vehicle, and SAH + MitoQ groups. Immunoprecipitation was performed using 2 μg polyclonal antibodies against mouse Nrf2 (ab89443). After a 3-h incubation, protein G sepharose was added and incubated overnight at 4 °C, and then centrifuged for 1 min at 12,000 × *g*. The precipitates were rinsed with immunoprecipitation buffer (0.5% NP 40, TrisCl pH 8.0, 0.15 M NaCl) four times to remove non-specific binding molecules. Sham extract without immunoprecipitation was used as input, while IgG was used as a negative control for precipitation. The protein levels of PHB2 in precipitates were then assessed by Western blot with anti-PHB2 (1: 500; ab15019).

2.10. Transmission electron microscopy

All rats were sacrificed and perfused with saline and 4% paraformaldehyde. We then prepared samples as previously described (Zhang et al., 2018). Briefly, the left temporal cortices were minced into small pieces (< 1 mm^3) and then fixed for 90 min. After dehydration, samples were embedded into araldite overnight at 60 °C. The specimens were then cut into 60-nm sections with an ultramicrotome (Leica, Norcross, GA, USA). Finally, the sections were fixed to nickel grids after staining. A transmission electron microscope (Carl Zeiss, Thornwood, NY, USA) was used for observation.

2.11. Assessment of mitochondrial proteins

Mitochondria isolation kit for tissue were both purchased from Thermo Fisher Scientific (Grand Island, NY, USA). The method for extraction was described previously (Qiu et al., 2011). Left basal cortical brain samples were equally divided into two parts for isolation of mitochondria respectively following the instruction manual. Western blot was then performed to detect the expression of the proteins of mitochondrial components.

2.12. Statistical analysis

All experiments were performed with full blinding, allocation concealment, and randomization. Before analysis, Shapiro-Wilk test was used to test the normality and variables were log transformed when necessary. Based on the distribution of normality, one-way analysis of variance (ANOVA) followed by the Tukey's *post-hoc* test was used when multiple group comparisons were involved (> 2 groups) with continuous independent variables, means ± SD were used for expression. If data was not normally distributed even with log transformation, Kruskal-Wallis test followed by the Dunn's *post-hoc* test was used for statistics, the medians (interquartile range) were used for expression. A p value of < 0.05 was defined as statistically significant. All statistical analyses were performed using SPSS 24.0 (IBM Corp., USA).

3. Results

3.1. Mortality and SAH severity scores

33 rats were part of the Sham group, 148 rats underwent SAH induction from which 5 rats were excluded. There was no mortality in the Sham group and the total mortality in SAH groups was 18.18% (26 of 143) (Fig. 1A). Subarachnoid blood clots were observed around the circle of Willis and ventral brainstem 24 h after SAH (Fig. 1B). There was no significant difference in average SAH grading scores among all of the SAH induced groups (Fig. 1C).

3.2. Time course expression of Nrf2, PHB2, OPA1 in EBI after SAH

Western blot expressions at 3, 6, 12, 24 and 72 h after SAH indicated that expression of Nrf2 rapidly increased to the peak at 3 h which was significantly higher than the Sham group, and then it gradually decreased until 72 h ($P < .05$; Fig. 2A, B). Additionally, PHB2 level after SAH declined and was notably lower than Sham group at both 24 h and 72 h ($P < .05$; Fig. 2A, C). Expression of long OPA1 (L-OPA1) after SAH was decreased until 72 h and was significantly lower than Sham group at 24 h and 72 h ($P < .05$; Fig. 2A, D). Expression of short OPA1 (S-OPA1) after SAH decreased until 24 h but the trend was not significant

A

Groups	Mortality rate	Excluded
Experiment 1		
(1) Sham	0% (0/9)	0
(2) SAH (3h,6h,12h,24h,72h)	21.43% (9/42)	1
Experiment 2		
(1) Sham	0% (0/6)	0
(2) SAH+vehicle	0% (0/6)	1
(3) SAH+MitoQ (1 mg/kg)	14.29% (1/7)	0
(4) SAH+MitoQ (3 mg/kg)	0% (0/6)	0
(5) SAH+MitoQ (9 mg/kg)	25% (2/8)	0
Experiment 3		
(1) Sham	0% (0/9)	0
(2) SAH+vehicle	25% (3/12)	0
(3) SAH+MitoQ (3 mg/kg)	10% (1/10)	0
(4) SAH+ML385+MitoQ	33.33% (3/9)	0
(5) SAH+DMSO+MitoQ	14.29% (1/7)	1
(6) SAH+PHB2 siRNA+MitoQ	14.29% (1/7)	0
(7) SAH+Scr siRNA+MitoQ	14.29% (1/7)	1
Experiemnt 4		
(1) Sham	0% (0/9)	0
(2) SAH+vehicle	18.18% (2/11)	0
(3) SAH+MitoQ (3 mg/kg)	18.18% (2/11)	1
Total		
Sham	0% (0/33)	
SAH	18.18% (26/143)	5

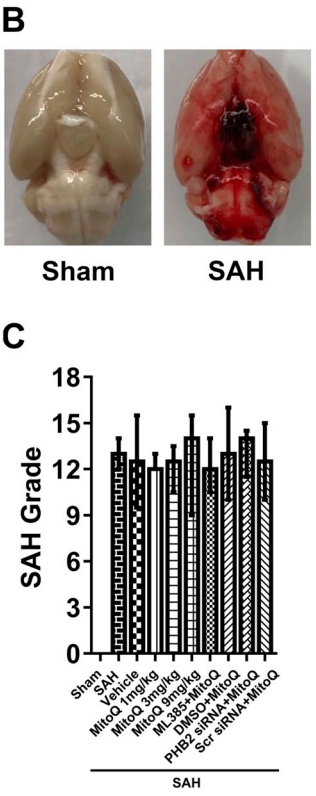

Fig. 1. Mortality rate and Subarachnoid hemorrhage (SAH) grade of Sham and SAH groups. (A) The number of mortality and excluded rats of each group (B) Schematic representation of Sham and SAH groups. (C) The SAH grade scores of the Sham and SAH groups. Data was expressed as the medians with interquartile range using Kruskal–Wallis test followed by the Dunn's *post-hoc* test.

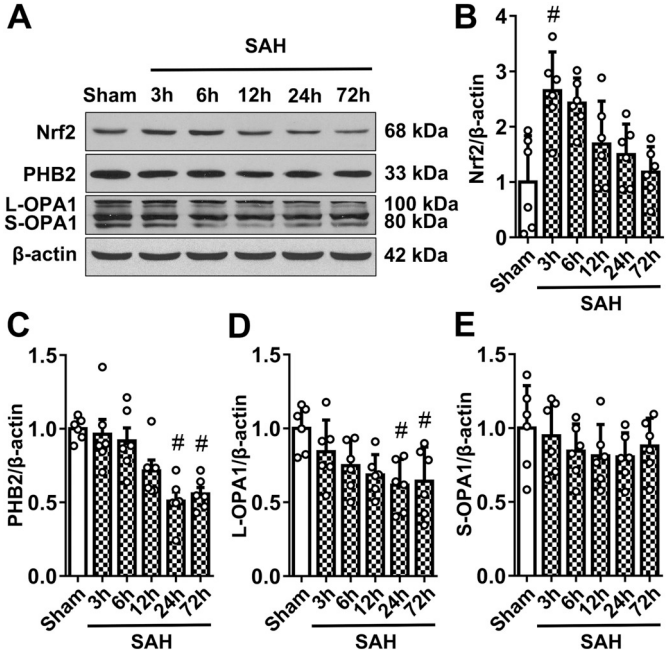

Fig. 2. Expression of endogenous NF-E2-related factor 2 (Nrf2), Prohibitin 2 (PHB2) and Optic Atrophy 1 (OPA1) after SAH.
(A) Representative Western blot bands and (B) quantitative analyses of Nrf2, PHB2 and OPA1 time course from the ipsilateral hemisphere 24 h after SAH. Relative densities of each protein have been normalized against the Sham group. n = 6 each group per time point. # $P < .05$ vs Sham. Data were expressed as the means with SD using one-way analysis of variance (ANOVA) followed by the Tukey *post-hoc* test.

($P > .05$; Fig. 2A, E).

Double immunofluorescence staining revealed Nrf2, PHB2 and OPA1 colocalizing with both astrocytes and endothelial cells at 24 h in SAH group (Fig. 3A, B) and Sham group (Supplemental Fig. II.).

3.3. MitoQ treatment improved Neurobehavior, attenuated brain edema

Modified Garcia, beam balance data, and brain water content indicated impairments in SAH + vehicle group when compared to Sham group ($P < .01$; Fig. 4A, B). MitoQ treated groups improved neurological scores and reduced brain water content when compared to SAH + vehicle group ($P < .05$; Fig. 4A-C, Supplemental Fig. III.). Since MitoQ (3 mg/kg) was superior to the other doses in measurements ($P < .05$; Fig. 4A-C), we chose 3 mg/kg as the best dosage of MitoQ and used it in following experiments.

3.4. MitoQ protected BBB disruption through Nrf2 and PHB2 dependent pathway

Western blot revealed no change in Nrf2, a significant decrease in expression of PHB2, OPA1 and Claudin-5, while increased expression of Albumin of SAH + vehicle group when compared with the Sham group ($P < .05$; Fig. 5A-G). Administration of MitoQ resulted in a significant increase of Nrf2, PHB2, L-OPA1 and Claudin-5, no change of S-OPA1, while decrease of Albumin when compared with SAH + vehicle group ($P < .05$; Fig. 5A-G).

Co-immunoprecipitation proved that the two proteins Nrf2 and PHB2 have interactions between each other. We also found that the binding extent of Nrf2/PHB2 followed a decreasing trend after SAH compared with Sham group ($P > .05$; Fig. 6A). However, when given MitoQ, the binding extent was reversed and increased when compared with SAH + vehicle group ($P < .05$; Fig. 6A).

3.5. Blockade of Nrf2 and PHB2 abolished the neuroprotection of MitoQ

Modified Garcia and beam balance tests showed that ML385 and PHB2 siRNA completely abolished the neuroprotective effects of MitoQ administration 24 h after SAH ($P < .05$; Fig. 6B, C).

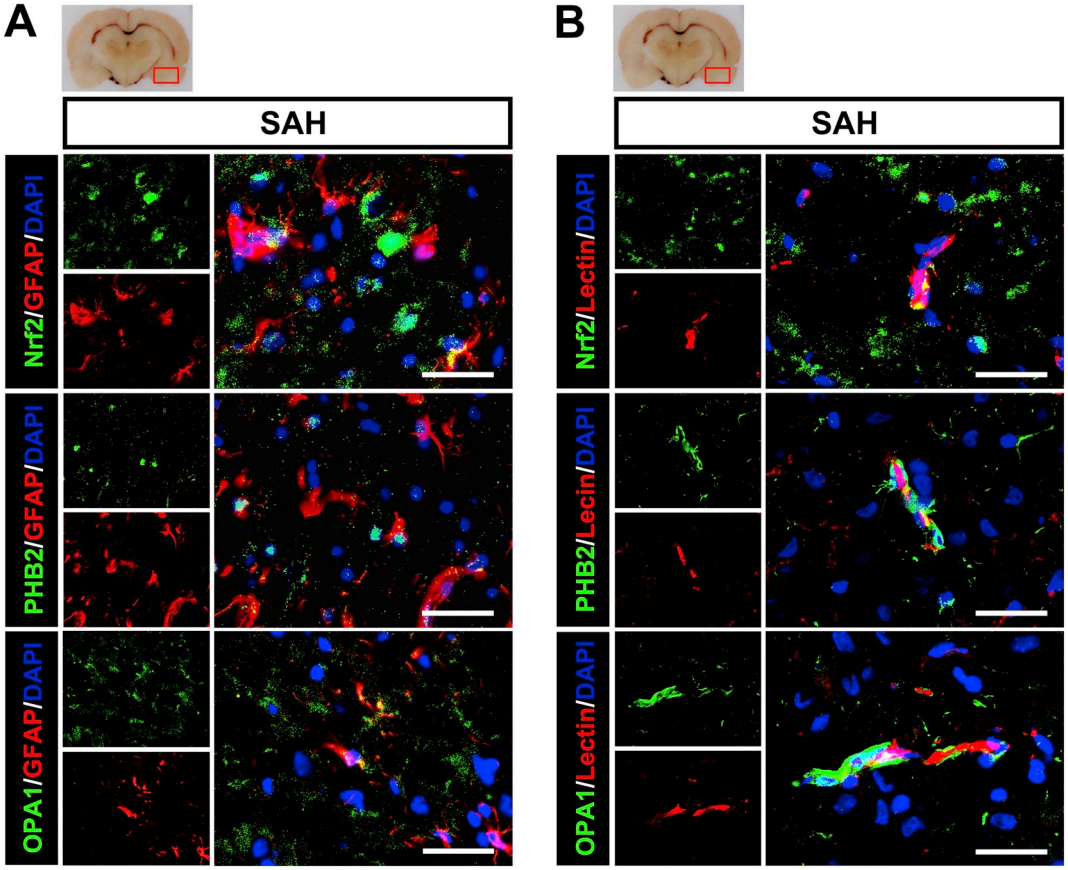

Fig. 3. Colocalizations of Nrf2, PHB2 and OPA1 24 h after subarachnoid hemorrhage (SAH).
Representative images of double immunofluorescence staining of Nrf2, PHB2 and OPA1 colocalized with (A) GFAP-positive astrocytes and (B) Lectin-positive endothelial cells at 24 h after SAH. n = 3 for each group. Scale bar = 50 μm. Red box of brain image presents region of interest. (For interpretation of the references to colour in this figure legend, the reader is referred to the web version of this article.)

Inhibition of Nrf2 with ML385 abolished effects of exogenous MitoQ, which led to decrease of Nrf2, PHB2, L-OPA1 and BBB disruption related proteins Claudin-5, while increase of Albumin compared with SAH + DMSO + MitoQ group ($P < .05$; Fig. 7A-G).

Downregulation of PHB2 and downstream L-OPA1, Claudin-5 while upregulation of Albumin occurred upon administration of PHB2 siRNA when compared to SAH + Scramble siRNA + MitoQ group ($P < .05$; Fig. 8A-G).

3.6. MitoQ protects mitochondria with an increase of PHB2 and OPA1

Transmission electron microscopy results demonstrated that when compared with Sham group, excessive mitochondrial swelling with vague cristae were found in the SAH + vehicle group (Fig. 9A). The SAH + MitoQ group presented with more normal mitochondria with a fusion state compared with SAH + vehicle group (Fig. 9A).

In mitochondrial extraction, expression of PHB2 and OPA1 was

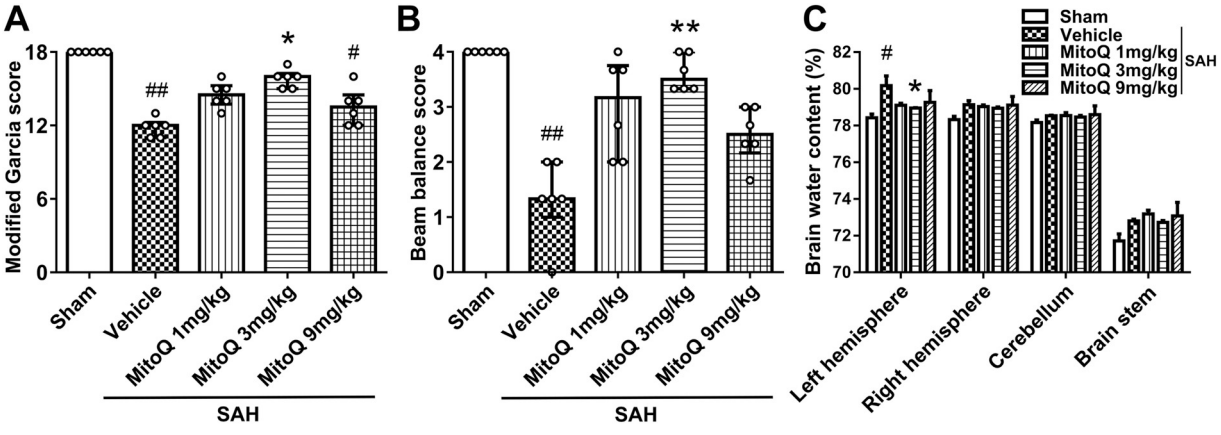

Fig. 4. Mitoquinone (MitoQ) attenuated neurological deficits and brain edema 24 h after SAH. (A) Modified Garcia, (B) beam balance scores and (C) brain water content of each part of each part of brain. n = 6 per group. # $P < .05$ vs. Sham group; ## $P < .01$ vs. Sham group. * $P < .05$ vs. SAH + vehicle group; ** $P < .01$ vs. SAH + vehicle group; Data of neurological scores were expressed as the medians with interquartile range using Kruskal–Wallis test followed by the Dunn's *post-hoc* test. Data of brain water content was expressed as the means with SD using ANOVA followed by the Tukey *post-hoc* test.

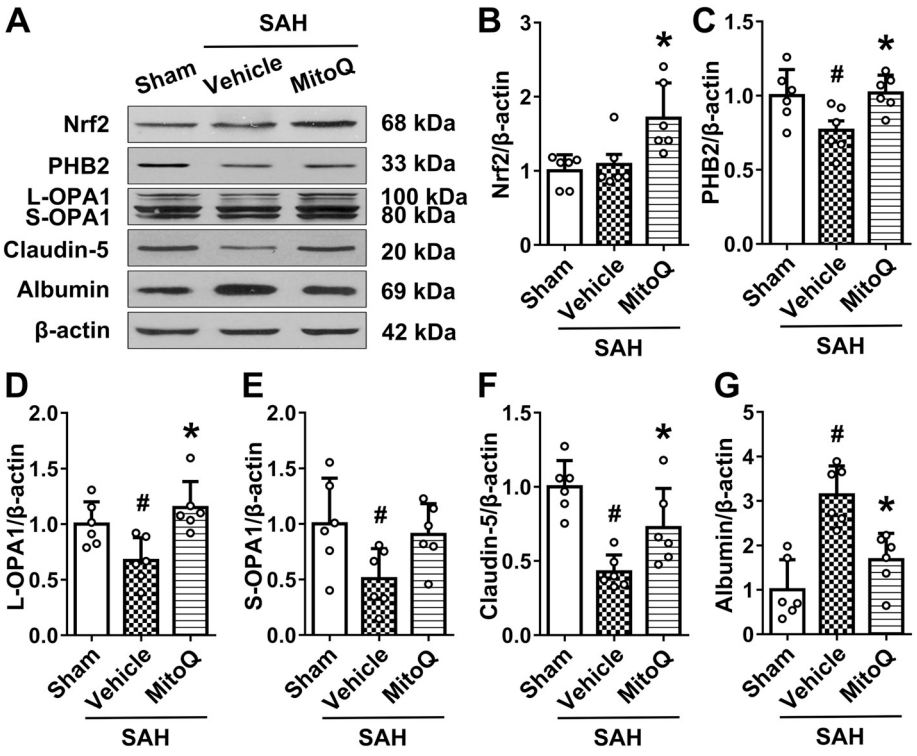

Fig. 5. The effect of MitoQ in protein expression of Nrf2, PHB2, long/short Optic Atrophy 1 (L-OPA1/S-OPA1), Claudin-5 and Albumin 24 h after SAH. (A) Representative Western blot images. Quantitative analyses of (B) Nrf2, (C) PHB2, (D) L-OPA1, (E) S-OPA1, (F) Claudin-5 and (G) Albumin. n = 6 per group. # $P < .01$ vs Sham group; * $P < .05$ vs SAH + vehicle group. Data were expressed as the means with SD using ANOVA followed by the Tukey *post-hoc* test.

significantly decreased in SAH + vehicle group compared to the Sham group ($P < .05$; Fig. 9B, C). However, MitoQ treatment group reversed expressions of these proteins compared with SAH + vehicle group ($P < .05$; Fig. 9B, C). In the cytoplasm, PHB2 and OPA1 were significantly increased in SAH + MitoQ group compared to the Sham group and also have a trend of increase compared to SAH + vehicle group ($P < .05$; Fig. 9D, E).

4. Discussion

In the present study, our findings revealed a transient increase of Nrf2 at 3 h SAH and a decrease in PHB2 and OPA1 at 24 h and 72 h time point of SAH. MitoQ treatment improved both neurological deficits and brain edema which is associated with upregulation of Nrf2, PHB2, OPA1, Claudin-5 and downregulation of Albumin. This study also proved that: (1) the upstream and downstream relationship of Nrf2 and PHB2 with co-immunoprecipitation. (2) Inhibition of Nrf2 abolished the improve outcomes with MitoQ, and pathway related proteins Nrf2, PHB2, OPA1, Claudin-5 were decreased while Albumin was increased. (3) Furthermore, knockdown of PHB2 in MitoQ treatment group had a similar manner of inhibition of Nrf2, which was associated with a decrease of PHB2, OPA1 and Claudin-5, while Albumin increased. (4) Lastly, we noted that there was an improvement of mitochondrial morphology and the increased expression of PHB2 and OPA1 in the mitochondrial extraction. Taken together, our findings suggest that MitoQ promotes attenuation of BBB disruption and associated improvement in neurological impairment through Nrf2/PHB2/OPA1 pathway after SAH.

MitoQ, a mitochondria-targeting drug which has a more specific and useful outcome compared with traditional antioxidant Coenzyme Q10

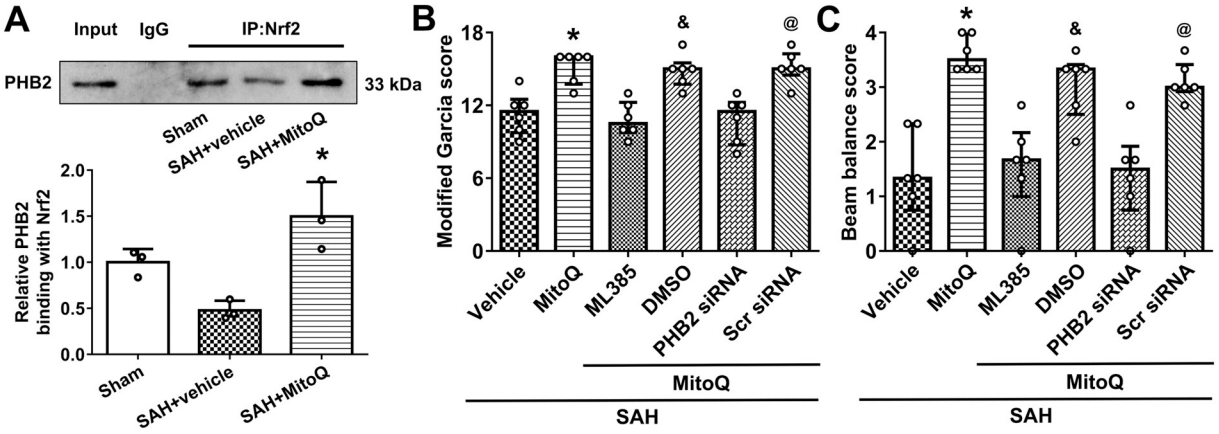

Fig. 6. MitoQ improved neurobehavior through Nrf2 and PHB2 dependent pathway 24 h after SAH. (A) Western blot images and quantitative analyses of PHB2 with co-immunoprecipitation of Nrf2 antibody in each group samples (# $P < .05$ vs. sham; * $P < .05$ vs. SAH + vehicle group; n = 3 per group). Data were expressed as the means with SD using ANOVA followed by the Tukey *post-hoc* test. (B) Modified Garcia and (C) beam balance scores in groups of mechanism study (* $P < .05$ vs. SAH + vehicle group; & $P < .05$ vs. SAH + ML385 + MitoQ group; @ $P < .05$ vs. SAH + PHB2 siRNA + MitoQ group; n = 6 per group). Data were expressed as the medians with interquartile range using Kruskal–Wallis test followed by the Dunn's *post-hoc* test.

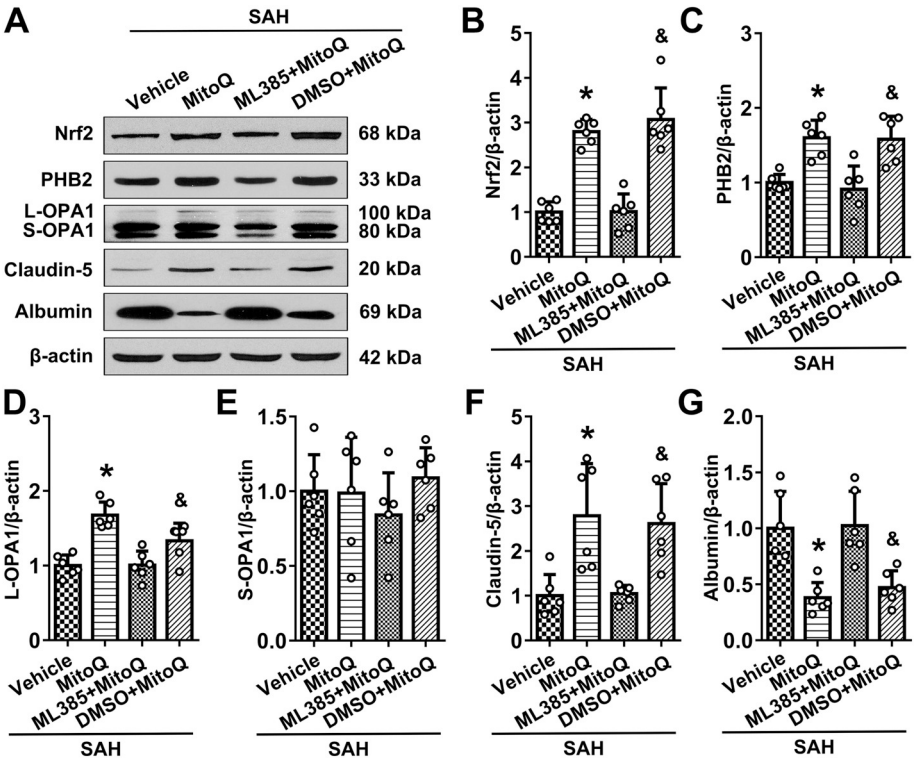

Fig. 7. Blokade of Nrf2 with ML385 abolished MitoQ treatment effects in blood brain barrier (BBB) protection 24 h after SAH. (A) Representative Western bolt images and quantitative analyses of (B) Nrf2, (C) PHB2, (D) L-OPA1, (E) S-OPA1, (F) Claudin-5 and (G) Albumin expressions. n = 6 per group. * $P < .05$ vs. SAH + vehicle group; & $P < .05$ vs. SAH + ML385 + MitoQ group. Data were expressed as the means with SD using ANOVA followed by the Tukey *post-hoc* test.

(Ham 3rd and Raju, 2017). Recently, MitoQ was indicated as an effective treatment in kidney injury and received extensive attention also in its neuroprotective effects (Xiao et al., 2017; Zhou et al., 2018). However, no research has been published to evaluate using MitoQ as a therapeutic method in SAH. In addition, liposoluble MitoQ can easily bypass the blood-brain barrier (Ham and Raju, 2017), In this study, we discovered that MitoQ treatment has the capacity to protect against BBB damage after SAH. At the same time, we found a reasonable mechanism for how MitoQ improves neurological function. However, choosing an appropriate dosage of MitoQ for clinical application is beneficial for future SAH patients. We used the method reported previously to set three different dosages in our experiments (Suzuki et al., 2018). In the

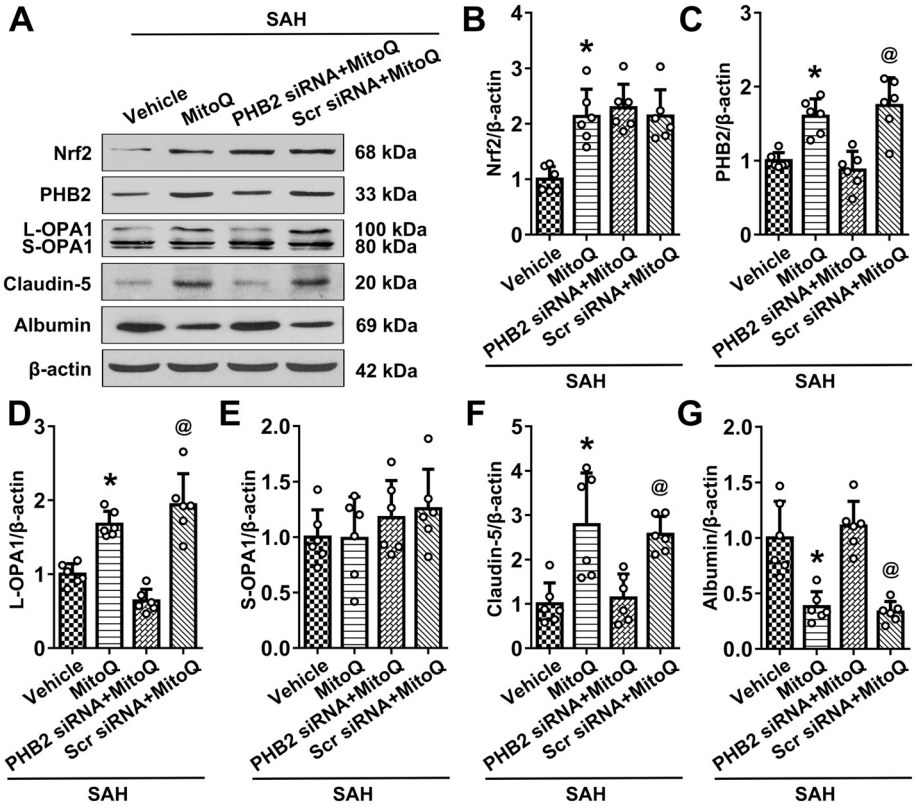

Fig. 8. Blokade of PHB2 with siRNA reversed the protective effects of MitoQ in BBB disruption 24 h after SAH. (A) Representative Western bolt images and quantitative analyses of (B) Nrf2, (C) PHB2, (D) L-OPA1, (E) S-OPA1, (F) Claudin-5 and (G) Albumin expressions. n = 6 per group. * $P < .05$ vs. SAH + vehicle group; @ $P < .05$ vs. SAH + PHB2 siRNA + MitoQ group. Data were expressed as the means with SD using ANOVA followed by the Tukey *post-hoc* test.

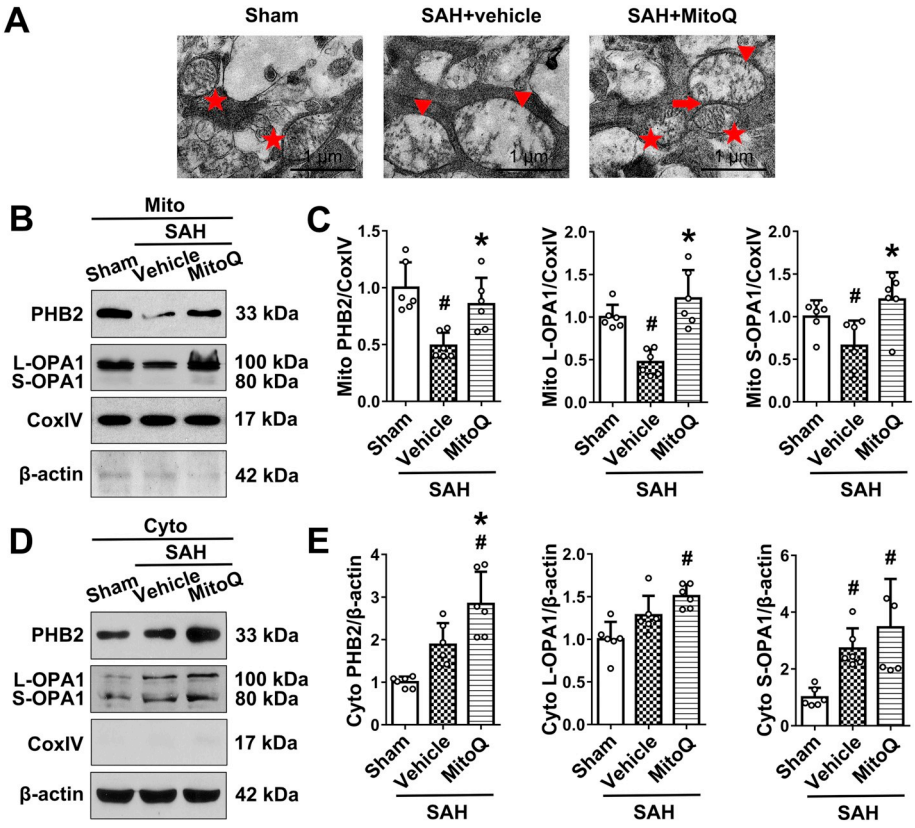

Fig. 9. The effects of Mitoquinone (MitoQ) on mitochondria after SAH. (A) Representative transmission electron microscopy images of each group on mitochondria (symbols indicate the following: asterisk = normal mitochondria; triangle = swelling and cristae vague; arrow = mitochondria under fusion; n = 3 for each group. Scale bars = 1 μm). (B, C) Western blot images and quantitative analyses of PHB2 and OPA1 mitochondrial extraction in each group. (D, E) Western blot images and quantitative analyses of PHB2 and OPA1 cytoplasmic extraction in each group (# $P < .05$ vs. sham; * $P < .05$ vs. SAH + vehicle group; n = 6 per group). Data were expressed as the means with SD using ANOVA followed by the Tukey *post-hoc* test.

result, 3 mg/kg of MitoQ is the most effective one for neurological recovery. The potential reason might be the low does (1 mg/kg) is not enough for the treatment effect, most of the drug may be metabolized during the blood circulation. And the worse outcome of high concentration (9 mg/kg) may refer to a previously reported concern that a pro-oxidant effect was associated with high concentrations of MitoQ (Doughan and Dikalov, 2007). Thus, 3 mg/kg of MitoQ was superior to other doses in measurements which may also valuable in the clinical study.

Brain edema is a significant component in the early stage of SAH, which could lead to many pathophysiological processes, such as BBB disruption (Pang et al., 2017). Previous studies proved that BBB permeability significantly increased during EBI, and both the structural and functional impairment of BBB integrity led to changes of vasogenic factors (Cao et al., 2016; Pang et al., 2017). A marked decline of Claudin-5 and elevation of Albumin are standard labels for detecting BBB disruption (Strecker et al., 2013). However, recent studies documented that Nrf2, an anti-oxidant related transcriptional regulator may serve as an upstream target to protect against BBB damage (Liu et al., 2016; Yu et al., 2018). Nrf2 activators were also demonstrated to be an effective treatment for CNS disorders (Imai et al., 2016; Liu et al., 2016). In this study, we were using MitoQ to protect against SAH-induced BBB disruption through upregulating Nrf2 expression as MitoQ has been proved to increase Nrf2 level by binding with its antagonistic protein Keap1.

Mitochondrial dysfunction plays an important role in the pathology of EBI (Chen et al., 2014). The processes of mitochondrial dynamics are thought to be crucial as a mechanism for the dysfunctional mitochondria (Reddy et al., 2011). Recently, most studies focused on the mitochondrial fission, the relations between fission related protein Drp1 and disruption of the BBB were addressed in TBI and SAH models (Fan et al., 2017; Wu et al., 2017). However, our recent study discovered mitochondrial fusion was also an essential component in the protection of SAH-induced outcome (Zhang et al., 2018). OPA1 especially the L-OPA1 is the main protein which associates with mitochondrial fusion and cristae structure (Civiletto et al., 2015; Lee et al., 2017). In this study, we targeted the proteolytic cleavage form L-OPA1 to S-OPA1 as this process is essential for mitochondrial fusion. We found that S-OPA1 did not change much in SAH-induced groups compared with Sham groups, while L-OPA1 had significantly decreased after SAH but recoverd or even express higher in MitoQ treatment group. These findings mean that although S-OPA1 could maintain mitochondrial morphology, L-OPA1 was more sensitive and vital in mitochondrial fusion.

PHB2 is a novel receptor of mitophagy, which is located in the inner membrane of mitochondria (Wei et al., 2017). Other than mitophagy, its role in mitochondrial dynamics has recently been discovered, in an optic atrophy model, OPA1 especially L-OPA1 isoforms were destabilized in PHB2-deficient cells, raising the possibility that PHB2 may act as an upstream of OPA1 (Osman et al., 2009). In our study, when we blocked PHB2 with siRNA, the expression of L-OPA1 was significantly decreased, which further supported the proposed pathway. When looking more upstream, previous studies indicated that the association of Nrf2 to brain mitochondria was involved in the protection of astrocytes (Narayanan et al., 2018), Nrf2 gene (NRF2) was related to PHB2 gene (Kakehashi et al., 2011), and OPA1 protein was also involved in Nrf2-mediated retrograde signaling pathway (Bertholet et al., 2013). Thus, we hypothesized that Nrf2 may serve as the upstream of MitoQ treatment mechanism. Co-immunoprecipitation and inhibition of Nrf2 both supported our previous stated hypothesis. Moreover, Co-immunoprecipitation indicated that Nrf2 can bind with PHB2 and also that there was an increase of Nrf2 and PHB2 binding in MitoQ treatment group compared with SAH + vehicle group. To some extent this discovery explained the changes of downstream proteins OPA1, Claudin-5, and Albumin.

Though our data robustly supports our hypothesis, our study did have some limitations. First, the mechanism of mitochondrial fusion is very complex; we only targeted one portion of the pathway. There may be other factors involved in MitoQ treatment, which need further

investigation. Second, MitoQ protective effects may be seen in other cell types such as neurons or microglia, because of this we plan to add these components into our future studies.

In conclusion, we demonstrated that MitoQ was able to attenuate BBB disruption through Nrf2/PHB2/OPA1 pathway in EBI after SAH, which is associated with improvement in neurological impairment. MitoQ may, therefore, be useful as a therapeutic medicine against neurological deficits in EBI after SAH.

Sources of funding

This study was supported by grants from NIH NS081740 and NS082184 to JHZ, a grant from China Postdoctoral Science Foundation [2018M630371] and a grant from Natural Science Foundation of Heilongjiang Province of China [ZD2018018].

Ethical approval

All procedures performed in studies involving animals were in accordance with the ethical standards of the institution or practice at which the studies were conducted.

Conflict of interest

The authors declare no conflict of interest.

Acknowledgments

None.

Appendix A. Supplementary data

Supplementary data to this article can be found online at https://doi.org/10.1016/j.expneurol.2019.02.009.

References

Bertholet, A.M., Millet, A.M., Guillermin, O., Daloyau, M., Davezac, N., Miquel, M.C., Belenguer, P., 2013. OPA1 loss of function affects in vitro neuronal maturation. Brain 136, 1518–1533.

Cao, S., Zhu, P., Yu, X., Chen, J., Li, J., Yan, F., Wang, L., Yu, J., Chen, G., 2016. Hydrogen sulfide attenuates brain edema in early brain injury after subarachnoid hemorrhage in rats: possible involvement of MMP-9 induced blood-brain barrier disruption and AQP4 expression. Neurosci. Lett. 621, 88–97.

Chen, S., Feng, H., Sherchan, P., Klebe, D., Zhao, G., Sun, X., Zhang, J., Tang, J., Zhang, J.H., 2014. Controversies and evolving new mechanisms in subarachnoid hemorrhage. Prog. Neurobiol. 115, 64–91.

Chen, Q., Shi, X., Tan, Q., Feng, Z., Wang, Y., Yuan, Q., Tao, Y., Zhang, J., Tan, L., Zhu, G., Feng, H., Chen, Z., 2017. Simvastatin promotes hematoma absorption and reduces hydrocephalus following Intraventricular Hemorrhage in part by Upregulating CD36. Transl. Stroke Res. 8, 362–373.

Civiletto, G., Varanita, T., Cerutti, R., Gorletta, T., Barbaro, S., Marchet, S., Lamperti, C., Viscomi, C., Scorrano, L., Zeviani, M., 2015. Opa1 overexpression ameliorates the phenotype of two mitochondrial disease mouse models. Cell Metab. 21, 845–854.

Claassen, J., Carhuapoma, J.R., Kreiter, K.T., Du, E.Y., Connolly, E.S., Mayer, S.A., 2002. Global cerebral edema after subarachnoid hemorrhage: frequency, predictors, and impact on outcome. Stroke 33, 1225–1232.

Doughan, A.K., Dikalov, S.I., 2007. Mitochondrial redox cycling of mitoquinone leads to superoxide production and cellular apoptosis. Antioxid. Redox Signal. 9, 1825–1836.

Fan, L.F., He, P.Y., Peng, Y.C., Du, Q.H., Ma, Y.J., Jin, J.X., Xu, H.Z., Li, J.R., Wang, Z.J., Cao, S.L., Li, T., Yan, F., Gu, C., Wang, L., Chen, G., 2017. Mdivi-1 ameliorates early brain injury after subarachnoid hemorrhage via the suppression of inflammation-related blood-brain barrier disruption and endoplasmic reticulum stress-based apoptosis. Free Radic. Biol. Med. 112, 336–349.

Fujii, M., Yan, J., Rolland, W.B., Soejima, Y., Caner, B., Zhang, J.H., 2013. Early brain injury, an evolving frontier in subarachnoid hemorrhage research. Transl. Stroke Res. 4, 432–446.

Gu, X., Zheng, C., Zheng, Q., Chen, S., Li, W., Shang, Z., Zhang, H., 2017. Salvianolic acid a attenuates early brain injury after subarachnoid hemorrhage in rats by regulating ERK/P38/Nrf2 signaling. Am. J. Transl. Res. 9, 5643–5652.

Ham 3rd, P.B., Raju, R., 2017. Mitochondrial function in hypoxic ischemic injury and influence of aging. Prog. Neurobiol. 157, 92–116.

Imai, T., Takagi, T., Kitashoji, A., Yamauchi, K., Shimazawa, M., Hara, H., 2016. Nrf2 activator ameliorates hemorrhagic transformation in focal cerebral ischemia under warfarin anticoagulation. Neurobiol. Dis. 89, 136–146.

Kakehashi, A., Ishii, N., Shibata, T., Wei, M., Okazaki, E., Tachibana, T., Fukushima, S., Wanibuchi, H., 2011. Mitochondrial prohibitins and septin 9 are implicated in the onset of rat hepatocarcinogenesis. Toxicol. Sci. 119, 61–72.

Korwitz, A., Merkwirth, C., Richter-Dennerlein, R., Troder, S.E., Sprenger, H.G., Quiros, P.M., Lopez-Otin, C., Rugarli, E.I., Langer, T., 2016. Loss of OMA1 delays neurodegeneration by preventing stress-induced OPA1 processing in mitochondria. J. Cell Biol. 212, 157–166.

Lee, H., Smith, S.B., Yoon, Y., 2017. The short variant of the mitochondrial dynamin OPA1 maintains mitochondrial energetics and cristae structure. J. Biol. Chem. 292, 7115–7130.

Liu, X., Zhang, X., Ma, K., Zhang, R., Hou, P., Sun, B., Yuan, S., Wang, Z., Liu, Z., 2016. Matrine alleviates early brain injury after experimental subarachnoid hemorrhage in rats: possible involvement of PI3K/Akt-mediated NF-kappaB inhibition and Keap1/Nrf2-dependent HO-1 inductionn. Cell. Mol. Biol. (Noisy-le-grand) 62, 38–44.

McManus, M.J., Murphy, M.P., Franklin, J.L., 2011. The mitochondria-targeted antioxidant MitoQ prevents loss of spatial memory retention and early neuropathology in a transgenic mouse model of Alzheimer's disease. J. Neurosci. 31, 15703–15715.

Narayanan, S.V., Dave, K.R., Perez-Pinzon, M.A., 2018. Ischemic preconditioning protects astrocytes against oxygen glucose deprivation via the nuclear erythroid 2-related factor 2 pathway. Transl. Stroke Res. 9, 99–109.

Osman, C., Merkwirth, C., Langer, T., 2009. Prohibitins and the functional compartmentalization of mitochondrial membranes. J. Cell Sci. 122, 3823–3830.

Pang, J., Chen, Y., Kuai, L., Yang, P., Peng, J., Wu, Y., Chen, Y., Vitek, M.P., Chen, L., Sun, X., Jiang, Y., 2017. Inhibition of blood-brain barrier disruption by an apolipoprotein E-mimetic peptide ameliorates early brain injury in experimental subarachnoid Hemorrhage. Transl. Stroke Res. 8, 257–272.

Pang, J., Peng, J., Matei, N., Yang, P., Kuai, L., Wu, Y., Chen, L., Vitek, M.P., Li, F., Sun, X., Zhang, J.H., Jiang, Y., 2018. Apolipoprotein E exerts a whole-brain protective property by promoting M1? Microglia quiescence after experimental subarachnoid hemorrhage in mice. Transl. Stroke Res. 9, 654–668.

Qiu, H., Lizano, P., Laure, L., Sui, X., Rashed, E., Park, J.Y., Hong, C., Gao, S., Holle, E., Morin, D., Dhar, S.K., Wagner, T., Berdeaux, A., Tian, B., Vatner, S.F., Depre, C., 2011. H11 kinase/heat shock protein 22 deletion impairs both nuclear and mitochondrial functions of STAT3 and accelerates the transition into heart failure on cardiac overload. Circulation 124, 406–415.

Reddy, P.H., Reddy, T.P., Manczak, M., Calkins, M.J., Shirendeb, U., Mao, P., 2011. Dynamin-related protein 1 and mitochondrial fragmentation in neurodegenerative diseases. Brain Res. Rev. 67, 103–118.

Strecker, J.K., Minnerup, J., Schutte-Nutgen, K., Gess, B., Schabitz, W.R., Schilling, M., 2013. Monocyte chemoattractant protein-1-deficiency results in altered blood-brain barrier breakdown after experimental stroke. Stroke 44, 2536–2544.

Sugawara, T., Ayer, R., Jadhav, V., Zhang, J.H., 2008. A new grading system evaluating bleeding scale in filament perforation subarachnoid hemorrhage rat model. J. Neurosci. Methods 167, 327–334.

Suzuki, H., Nakatsuka, Y., Yasuda, R., Shiba, M., Miura, Y., Terashima, M., Suzuki, Y., Hakozaki, K., Goto, F., Toma, N., 2018. Dose-dependent inhibitory effects of Cilostazol on delayed cerebral infarction after aneurysmal subarachnoid Hemorrhage. Transl. Stroke Res. https://doi.org/10.1007/s12975-018-0650-y. (Epub ahead of print).

Wei, Y., Chiang, W.C., Sumpter Jr., R., Mishra, P., Levine, B., 2017. Prohibitin 2 is an inner mitochondrial membrane mitophagy receptor. Cell 168 (224–238), e210.

Wu, P., Li, Y., Zhu, S., Wang, C., Dai, J., Zhang, G., Zheng, B., Xu, S., Wang, L., Zhang, T., Zhou, P., Zhang, J.H., Shi, H., 2017. Mdivi-1 alleviates early brain injury after experimental subarachnoid Hemorrhage in rats, possibly via inhibition of Drp1-activated mitochondrial fission and oxidative stress. Neurochem. Res. 42, 1449–1458.

Xiao, L., Xu, X., Zhang, F., Wang, M., Xu, Y., Tang, D., Wang, J., Qin, Y., Liu, Y., Tang, C., He, L., Greka, A., Zhou, Z., Liu, F., Dong, Z., Sun, L., 2017. The mitochondria-targeted antioxidant MitoQ ameliorated tubular injury mediated by mitophagy in diabetic kidney disease via Nrf2/PINK1. Redox Biol. 11, 297–311.

Yan, J., Li, L., Khatibi, N.H., Yang, L., Wang, K., Zhang, W., Martin, R.D., Han, J., Zhang, J., Zhou, C., 2011. Blood-brain barrier disruption following subarchnoid hemorrhage may be faciliated through PUMA induction of endothelial cell apoptosis from the endoplasmic reticulum. Exp. Neurol. 230, 240–247.

Yu, Z., Lin, L., Jiang, Y., Chin, I., Wang, X., Li, X., Lo, E.H., Wang, X., 2018. Recombinant FGF21 protects against blood-brain barrier leakage through Nrf2 Upregulation in type 2 diabetes mice. Mol. Neurobiol. https://doi.org/10.1007/s12035-018-1234-2. (Epub ahead of print).

Zhang, T., Wu, P., Zhang, J.H., Li, Y., Xu, S., Wang, C., Wang, L., Zhang, G., Dai, J., Zhu, S., Liu, Y., Liu, B., Reis, C., Shi, H., 2018. Docosahexaenoic acid alleviates oxidative stress-based apoptosis via improving mitochondrial dynamics in early brain injury after subarachnoid hemorrhage. Cell. Mol. Neurobiol. 38, 1413–1423.

Zhou, J., Wang, H., Shen, R., Fang, J., Yang, Y., Dai, W., Zhu, Y., Zhou, M., 2018. Mitochondrial-targeted antioxidant MitoQ provides neuroprotection and reduces neuronal apoptosis in experimental traumatic brain injury possibly via the Nrf2-ARE pathway. Am. J. Transl. Res. 10, 1887–1899.